High-Temperature Single-Crystal X-ray Diffraction Studies of Potassium and (Cesium, Potassium) Titanyl Arsenates

Paul A. Northrup and John B. Parise

Department of Earth and Space Sciences, State University of New York at Stony Brook, Stony Brook, New York 11794-2100

L. K. Cheng, L. T. Cheng, and E. M. McCarron

Science and Engineering Laboratory, E. I. DuPont de Nemours & Co., Experimental Station, P.O. Box 80306, Wilmington, Delaware 19880-0306

Received October 22, 1993. Revised Manuscript Received February 1, 1994[⊛]

The crystal structures of the nonlinear optical materials $KTiOAsO_4$ (KTA) and $(Cs_{0.6}K_{0.4})TiOAsO_4$ ((Cs,K)TA) have been studied at room temperature and up to 725 and 550 °C, respectively. With increasing temperature, the *a* and *b* cell dimensions and unit-cell volumes increase while *c* decreases. Although the unit-cell volume for (Cs,K)TA is larger than that for KTA, the *c* parameter is smaller. For KTA, the mean linear thermal expansion coefficients along *a*, *b*, and *c* are 1.29, 1.58, and -0.65×10^{-5} K^{-1}, respectively, in the temperature range studied. The volumetric thermal expansion coefficient is 2.34×10^{-5} K^{-1}. The corresponding values for $(Cs_{0.6}K_{0.4})TiOAsO_4$ are 1.20×10^{-5}, 3.06×10^{-5}, and -1.52×10^{-5} K^{-1} and 2.68×10^{-5} K^{-1}. In (Cs,K)TA the Cs is strongly partitioned into the larger of two extraframework cation sites below 500 °C but disorders above this temperature. Structure models refined at several intermediate temperatures showed significant changes in the potassium/cesium environment, and a reduction of distortion within the titanium octahedra. Polyhedral rotations within the corner-linked framework are related to a negative thermal expansion along *c*. Tilt angles θ and ϕ, defined for the AsO_4 tetrahedra as inclination of an O–O edge to the *a* or *b* axis, increase as functions of both temperature and cation size. The structural trends are consistent with the onset of a phase transition from orthorhombic space group $Pna2_1$ to $Pnan$ at higher temperatures.

Introduction

$KTiOPO_4$ (KTP) and its derivatives form an isostructural family of both technological and academic interest within the field of applied nonlinear optics (NLO).[1] An excellent review of the KTP structure field is given by Stucky et al.[2] $KTiOAsO_4$ (KTA) is an important member of this structure family, with certain advantageous as well as complementary properties to those of KTP. In particular, KTA is reported[3] to have a higher SHG coefficient and to be well-suited for applications at infrared wavelengths.[4] Furthermore, the electrooptic properties of Cs-substituted titanyl arsenates may even surpass those of KTA.[5,6]

The structure of KTA, shown in Figure 1, consists of corner-linked undulating chains of octahedrally coordinated Ti parallel to [011] and [01$\bar{1}$]. These are cross-linked by arsenate tetrahedra, forming a three-dimensional framework. The octahedral chains are unusual in that they contain an alternation of long (single) and short
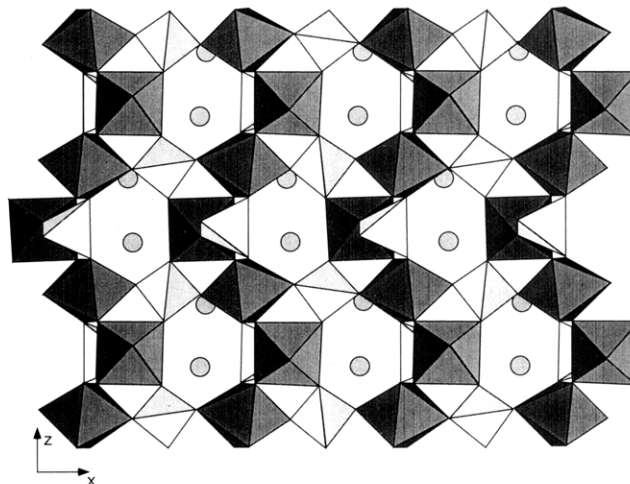

Figure 1. Plot of KTA structure at 20 °C, viewed down *b*.

(double) Ti–O bonds. This feature is believed to be responsible for the NLO properties.[5] Potassium ions occupy openings in the framework, which form channels in the [001] and [100] directions. The large ionic conductivity especially in the [001] direction of KTP and its derivatives is a consequence of the presence of these channels.[2] Thus cation-exchange reactions can be readily used to alter the composition and properties of the material.[5]

The effects of framework and cation composition on this structure have been extensively studied.[2,5,7] Very little work, however, has been done involving the effects of temperature on structure. KTA and (Cs,K)TA both

[⊛] Abstract published in *Advance ACS Abstracts,* March 1, 1994.

(1) Bolt, R. J. Crystal Growth and Characterization of Potassium Titanyl Phosphate and Barium Metaborate, Ph.D. Thesis; University of Nijmegen: The Neterlands, 1992.

(2) Stucky, G. D.; Phillips, M. L. F.; Gier, T. E. *Chem. Mater.* **1989,** *1,* 492.

(3) Bierlein, J. D.; Vanherzeele, H.; Ballman, A. A. *Appl. Phys. Lett.* **1989,** *54,* 783. See also erratum: *Appl. Phys. Lett.* **1992,** *61,* 3193.

(4) Cheng, L. K.; Bierlein, J. D.; Ballman, A. A. *J. Cryst. Growth* **1991,** *110,* 697.

(5) Phillips, M. L. F.; Harrison, W. T. A.; Stucky, G. D.; McCarron, E. M. III; Calabrese, J. C.; Gier, T. E. *Chem. Mater.* **1992,** *4,* 222.

(6) Cheng, L. K.; Cheng, L. T.; Zumsteg, F. C.; Bierlein, J. D.; Galperin, J. J. *Cryst. Growth.* in press.

Potassium and (Cesium, Potassium) Titanyl Arsenates

Chem. Mater., Vol. 6, No. 4, 1994 435

crystallize in space group $Pna2_1$ at room temperature. At elevated temperature, they undergo a phase transition to a centrosymmetric structure, as evidenced by the disappearance of the NLO properties. The ferroelectric to paraelectric Curie temperature (T_c) for the transition in KTA is 880 °C;[3,8] in (Cs,K)TA it is lower, estimated in this work at about 780 °C. Previously, Harrison et al.[9] found that thallium titanyl phosphate (TTP) transformed to $Pnan$ symmetry at ~600 °C. The present study examines several aspects of the structure and chemistry of KTiO-AsO$_4$ and (Cs$_{0.6}$K$_{0.4}$)TiOAsO$_4$, as a function of temperature. The relative influences of cation size and of temperature are compared and contrasted in order to better understand the dynamics of the titanyl arsenate framework.

Experimental Section

The KTA sample was obtained in the following manner: A sample of 30 g of a glass of stoichiometry KTiAsO$_5$ was made by heating the appropriate amounts of KOH, TiO$_2$, and As$_2$O$_5$ to 1000 °C for 3 h and subsequently quenching the sample by pouring it onto an Al plate. Using this glass as nutrient, crystals of KTiOAsO$_4$ were grown hydrothermally in sealed gold tubes at 3 kbar. The gold tubes were initially heated to 700 °C for 3 h and then cooled in such a way that a gradient was established between the nutrient (600 °C) and the growth (550 °C) zones. Growth runs typically ran for 48–72 h producing millimeter-sized crystals. Twelve crystals, 0.2–0.3 mm in size, were chosen for uniformity of shape and crystalline quality. Those selected were nearly equidimensional, transparent, clean, and optically uniform. Sharp, single diffraction peaks were verified by scans ($\omega/2\theta$ and ω) performed on all crystals. Samples were mounted on quartz glass fibers with high-temperature cement and placed in a modified single-crystal heater on a Picker four-circle diffractometer.[10-12]

The heater consists of a two-prong heating element encased in refractory cement, which is suspended over the crystal and mounted to the χ-circle to move with the crystal. A thermocouple is situated less than 1 mm above the crystal position. This assembly is surrounded by a Kapton plastic enclosure, which seals to the crystal mount.

The (Cs,K)TA crystals were obtained by flux growth. A mixture of 133 g of Cs$_2$CO$_3$, 14 g of K$_2$CO$_3$, 21.6 g of TiO$_2$, and 82.7 g of As$_2$O$_5$ was fired in a 100-mL platinum crucible at 1050 °C and then cooled at ~5 °C/h to 700 °C. The resulting crystals were found to be Cs$_{0.57}$K$_{0.42}$TiOAsO$_4$ by inductively coupled plasma spectrometry. This is in good agreement with site occupancy factors refined from X-ray diffraction data described below. Much of this material showed fine-scale optic domains, perhaps because of twinning or intergrowth. Small pieces and cleavage fragments were examined for suitability as single-crystal samples. The one chosen was equidimensional, approximately 0.15 mm across, transparent, and optically uniform. Several diffraction peaks were scanned; they were single and sharp.

Unit cell parameters for KTA and (Cs,K)TA were determined at several temperatures from 7 to 24 reflections, centered at ±2θ, between 30 and 35°. Figure 2 shows the measured unit cell parameters as a function of temperature. Variations in temperature are within ±6 °C (1%). Data sets were collected at 20, 505, 630, and 725 °C for KTA using two crystals and at 20, 220, 400, 550, and 700 °C for one (Cs,K)TA sample. Intensities were
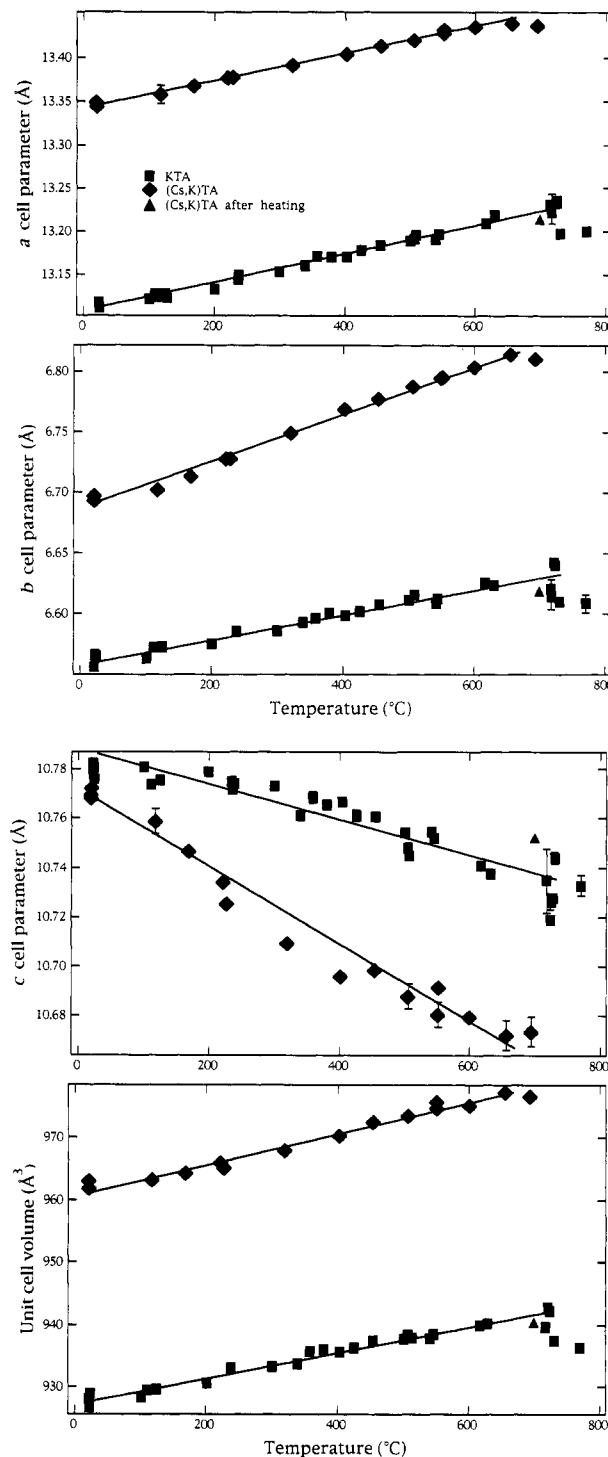
Figure 2. Unit-cell parameters for KTA and (Cs,K)TA as a function of temperature (data compiled from several crystals). Includes unit-cell parameters of (Cs,K)TA after 48 h at 700 °C. Errors are within the size of the markers unless otherwise indicated.

measured using a constant precision method[13] in which the collection time for each peak was adjusted to achieve a specified precision ($\sigma(I)/I$). A maximum time of 150 s was allowed to achieve this value. At higher temperatures, some precision was sacrificed for faster collection of data. Table 1 summarizes the data collection and structure refinement parameters. Unit weights were used so as to preserve the large number of weak reflections important to this study.

(7) Crennell, S. J.; Morris, R. E.; Cheetham, A. K.; Jarman, R. H.; *Chem. Mater.* **1992**, *4*, 82.

(8) Yanovskii, V. K.; Voronkova, V. I. *Phys. Status Solidi A* **1980**, *93*, 665.

(9) Harrison, W. T. A.; Gier, T. E.; Stucky, G. D.; Schulz, A. J. *J. Chem. Soc., Chem. Commun.* **1990**, *7*, 540.

(10) Northrup, P. High Temperature Single-Crystal X-Ray Diffraction Studies of K- and (Cs,K)-TiOAsO$_4$, M.S. Thesis, State University of New York, Stony Brook, NY, 1993.

(11) Brown, G. E.; Sueno, S.; Prewitt, C. T. *Am. Miner.* **1973**, *58*, 698.

(12) Parise, J. B.; Corbin, D. R.; Abrams, L.; Northrup, P.; Rakovan, J.; Nenoff, T. M.; Stucky, G. D. *Zeolites* **1994**, *14*, 25.

(13) Finger, L. W.; Baldwin, K. J. *The single-crystal diffractometer control programs for the PDP11/44 computer*; Department of Earth and Space Sciences, State University of New York at Stony Brook, 1985.

Table 1. Summary of Data Collection and Structure Refinement Parameters for KTA and (Cs,K)TA

	KTA				CTA			
temp (°C)[a]	19–22	502–512	623–639	718–729	19–22	219–225	398–405	547–557
sample	8	10	8	10	1			
space group	$Pna2_1$				$Pna2_1$			
Z	8				8			
formula wt	241.91				300.1			
a (Å)	13.1185(5)	13.1924(20)	13.2185(11)	13.2386(23)	13.3441(12)	13.3782(29)	13.4045(36)	13.4313(36)
b (Å)	6.5656(2)	6.6172(13)	6.6234(9)	6.6417(12)	6.6935(5)	6.7281(10)	6.7689(10)	6.7955(16)
c (Å)	10.7804(3)	10.7450(19)	10.7374(10)	10.7189(17)	10.7689(9)	10.7336(22)	10.6960(12)	10.6911(21)
vol (Å³)	928.5	938.0	940.1	942.5	961.9	966.1	970.5	975.8
calcd density (g/cm³)	3.463	3.426	3.419	3.410	4.15	4.13	4.11	4.09
μ(Mo) (cm⁻¹)	97.1	96.0	95.8	95.6	146.1	145.5	144.8	144.1
radiation	Mo Kα				Mo Kα			
scan method	$\omega/2\theta$				$\omega/2\theta$			
2θ range (deg)	5–60	5–55	5–65	5–55	5–60	5–50	5–60	5–45
data octants	+++,++−	+++,++−	+++,++−	+++,++−	+++,++−	+++,++−	+++,++−	+++,++−
max h,k,l	18,9,15	17,9,14	20,10,16	17,9,14	18,9,15	15,7,12	18,9,15	14,7,11
diffraction peaks collected	2726	1577	3414	1592	3032	1841	3020	747
unique data ($I > 2.5\sigma I$)	2678	1490	2978	1341	2823	1711	2638	655
abs method	spherical	Gaussian	spherical	Gaussian	Gaussian			
transmission range	0.249–0.270	0.155–0.284	0.252–0.273	0.156–0.286	0.2353–0.2505	0.2368–0.2521	0.2384–0.2598	0.2399–0.2521
refinement method	full matrix least squares on F				full matrix least squares on F			
weighting scheme	unit				unit			
atoms refined	all anisotropic				all anisotropic			
params varied	144				146			
param/data ratio	18.6	10.3	20.7	9.3	19.3	11.7	18.1	4.5
R^b	0.022	0.052	0.045	0.056	0.032	0.037	0.048	0.040
$R_w{}^b$	0.026	0.064	0.048	0.066	0.035	0.044	0.049	0.041
error of fit[b]	1.42	1.58	2.06	1.61	1.09	2.92	2.50	2.61
sec ext coeff	0.72(2)	0.58(2)	0.50(2)	0.8(1)	0.23(2)	0.36(2)	0.34(2)	0.26(8)

[a] Temperature ranges given are the outer limits of observed variations due to crystal position, plus the calibration uncertainty. [b] $R = \Sigma(F_o - F_c)/\Sigma(F_o)$, $R_w = [\Sigma(w(F_o - F_c)^2)/\Sigma(wF_o^2)]^{1/2}$ and error of fit $= [\Sigma(w(F_o - F_c)^2)/(\text{no. of reflns} - \text{no. of params})]^{1/2}$.

Several test reflections were collected at intervals during heating to monitor the onset of the phase transition from $Pna2_1$ to $Pnan$. These sets included several of both standard reflections (those present in both space groups) and [$hk0, h + k = 2n + 1$] reflections which should become extinct at the transition. No data could be collected above the phase transition, however; overall intensity decreased to zero very quickly above 800 °C in KTA due to decomposition, and compositional change occurred in (Cs,K)TA above 550 °C. Observations of (Cs,K)TA in the interval 550–750 °C indicated that both structure and composition were changing over time, as discussed below. In this temperature range, initial observations indicated substantial weakening of the [$hk0, h + k = 2n + 1$] reflections. However, in the approximately 80 min taken to update cell parameters and orientation and to collect quantitative data on the test set of reflections, those reflections *regained* intensity, clearly indicating persistence of the $Pna2_1$ symmetry. At 700 °C, the cell parameters changed dramatically, becoming comparable to those of pure KTA at that temperature (Figure 2).

Structure refinements were carried out using the NRCVAX software package.[14] For all temperatures and both compositions, 144–146 parameters (16 atoms) were refined, unit weights were used, and Fourier difference maps were checked for extraneous peaks. Since the space group is noncentrosymmetric, the polarity was identified for each crystal. The room-temperature structure determined by El Brahimi and Durand[15] was used as a starting model for the KTA data sets. Fractional atomic coordinates, anisotropic thermal parameters, and a secondary extinction coefficient were refined for the 20 °C data. Each refinement began with the previous lower temperature structure model. Refined atomic parameters are given in Table 2 for KTA at each temperature. The refined KTA structure at 20 °C was used as a starting model for the (Cs,K)TA data; atomic positions and Cs/K occupancy factors were determined first. Table 3 contains the refined atomic parameters of (Cs,K)TA at 22, 220, 400, and

(14) Gabe, E. J.; Le Page, Y.; Charland, J. P.; Lee, F. L. *The NRCVAX Structure System*; Chemistry Division, NRC: Ottawa, Canada, 1989.

(15) El Brahimi, M.; Durand, J. *Rev. Chem. Miner.* **1986**, *23*, 146.

(16) Johnson, C. K. *ORTEP: A fortran thermal-ellipsoid plot program for crystal structure illustrations, Report ORNL-3794*. Oak Ridge National Laboratory, 1965.

550 °C. The 700 °C data proved to be unrefineable, due to continuous changes in structure and composition.

Results and Discussion

A significant structural change occurs within the Ti octahedra as temperature increases. The highly distorted octahedra become much more symmetric at increased temperatures. Stucky et al.[2] defined the asymmetry, Δ, as the difference in length between the long and short *trans*-Ti–O bonds. While the exact mechanism is still debated,[5] the NLO properties of KTP are believed to be related to this distortion, the asymmetry of the O—Ti=O bond chain. There is evidence[2,9] that both NLO properties and Δ decrease with increasing temperature in the KTP family. In KTA, Δ was found to decrease significantly above 500 °C (Figure 3). The changes in Δ, however, appear to be relatively independent of the framework rotations described below. Moreover, structural changes resulting from cation size differences alone do not systematically effect Δ.

While ΔTi(2) decreases to zero, Δ Ti(1) fails to decrease more than 50%, even in TTP above its T_c.[2] This observation prompted a closer look at the Ti(1) octahedron (Figure 4). ΔTi(1) is calculated from the lengths of the *trans*-(Ti–O) bonds, one of which is connected to a TiO₆ octahedron and the other to an AsO₄ tetrahedron. It is therefore unlikely that ΔTi(1) will ever equal zero. At the phase transition in both materials studied the Ti(1) atom does not move to the center of its octahedral coordination, but rather to a position on a plane of symmetry lying between the *cis* oxygens (Figure 4). However, for the phase transition to the centrosymmetric structure, ΔTi(1) need not be zero; the individual polarities of the *trans*-Ti–O bonds become oriented in opposing pairs with no net (bulk) nonlinearity. Δ_cTi(1) (defined here as the difference in

Table 2. Refined Atomic Coordinates and Thermal Parameters for KTA[a]

	x	y	z	B_{iso}
	(a) Sample 8 and 20 °C			
K1	0.3766(1)	0.7791(2)	0.3129(2)	1.74(5)
K2	0.1079(1)	0.7000(2)	0.0684(2)	1.67(5)
Ti1	0.3748(1)	0.5065(2)	0.00000	0.37(3)
Ti2	0.2467(1)	0.2714(1)	0.2493(2)	0.36(3)
As1	0.49790(4)	0.3290(1)	0.2591(2)	0.33(2)
As2	0.18113(3)	0.5071(1)	0.5118(1)	0.36(2)
O1	0.9878(4)	0.0026(8)	0.1437(5)	0.77(14)
O2	0.5067(4)	0.4612(8)	0.3920(5)	0.89(15)
O3	0.3937(3)	0.1819(6)	0.2765(5)	0.68(15)
O4	0.0984(3)	0.3268(7)	0.2383(5)	0.68(14)
O5	0.3924(3)	0.8054(7)	0.0466(4)	0.66(15)
O6	0.6053(3)	0.7945(7)	0.4828(5)	0.84(15)
O7	0.2391(4)	0.0414(8)	0.1319(5)	0.74(15)
O8	0.2592(4)	0.4651(8)	0.3898(5)	0.77(15)
OT1	0.2163(4)	0.0545(8)	0.3885(5)	0.77(14)
OT2	0.2789(4)	0.4574(8)	0.1393(5)	0.66(14)
	(b) Sample 10 at 500 °C			
K1	0.3811(6)	0.7819(10)	0.3321(11)	6.8(4)
K2	0.1083(5)	0.7019(10)	0.0856(10)	5.9(4)
Ti1	0.8736(2)	0.9963(4)	0.00000	1.2(1)
Ti2	0.2495(2)	0.2664(4)	0.2501(5)	1.2(1)
As1	0.4995(1)	0.3277(2)	0.2577(5)	1.12(4)
As2	0.1801(1)	0.5029(2)	0.5107(4)	1.19(4)
O1	0.9889(13)	0.014(3)	0.1375(17)	2.5(6)
O2	0.5081(11)	0.467(4)	0.3848(19)	2.9(7)
O3	0.3956(10)	0.182(2)	0.2773(18)	2.3(6)
O4	0.1008(9)	0.324(2)	0.2343(15)	1.7(5)
O5	0.3910(9)	0.804(2)	0.0508(17)	2.3(6)
O6	0.6082(13)	0.795(2)	0.4781(16)	2.7(6)
O7	0.2407(10)	0.040(3)	0.1334(16)	2.4(6)
O8	0.2583(13)	0.459(3)	0.3895(17)	2.8(6)
OT1	0.2195(12)	0.053(3)	0.3885(15)	1.9(5)
OT2	0.2805(12)	0.454(3)	0.1396(15)	2.1(5)
	(c) Sample 8 at 630 °C			
K1	0.3821(6)	0.7831(8)	0.3366(10)	9.4(4)
K2	0.1086(5)	0.7024(10)	0.0881(9)	8.2(4)
Ti1	0.8731(1)	0.9971(4)	0.0000	1.63(6)
Ti2	0.2506(2)	0.2626(3)	0.2508(4)	1.70(5)
As1	0.4998(1)	0.3278(1)	0.2559(4)	1.48(3)
As2	0.1801(1)	0.5014(2)	0.5083(3)	1.55(3)
O1	0.9883(10)	0.023(3)	0.1317(14)	3.4(6)
O2	0.5124(12)	0.476(3)	0.3813(16)	3.6(6)
O3	0.3959(8)	0.186(2)	0.2792(15)	3.2(5)
O4	0.0998(6)	0.327(1)	0.2350(11)	2.0(4)
O5	0.3934(8)	0.803(1)	0.0457(12)	2.5(4)
O6	0.6076(10)	0.797(2)	0.4771(14)	3.6(5)
O7	0.2420(11)	0.040(2)	0.1296(12)	2.8(4)
O8	0.2604(10)	0.460(2)	0.3907(13)	3.3(5)
OT1	0.2168(10)	0.048(2)	0.3825(14)	2.7(5)
OT2	0.2804(9)	0.448(2)	0.1319(13)	2.4(4)
	(d) Sample 10 at 725 °C			
K1	0.3816(11)	0.785(2)	0.347(2)	12.4(12)
K2	0.1077(8)	0.706(3)	0.094(2)	11.4(12)
Ti1	0.3725(2)	0.501(1)	0.0000	2.1(2)
Ti2	0.2505(5)	0.251(1)	0.2526(11)	2.3(1)
As1	0.5006(2)	0.3278(2)	0.2540(9)	1.86(5)
As2	0.1798(1)	0.4987(5)	0.5034(9)	1.9(1)
O1	0.9892(16)	0.017(6)	0.129(4)	6.0(13)
O2	0.5172(12)	0.477(3)	0.378(2)	2.4(6)
O3	0.3986(13)	0.183(4)	0.286(2)	2.7(7)
O4	0.1033(15)	0.324(3)	0.241(2)	2.6(7)
O5	0.3927(11)	0.801(3)	0.042(2)	2.5(7)
O6	0.6126(23)	0.798(4)	0.468(3)	6.6(15)
O7	0.2445(14)	0.037(4)	0.125(2)	3.2(8)
O8	0.2617(16)	0.456(4)	0.380(3)	4.0(10)
OT1	0.2152(17)	0.055(3)	0.372(3)	2.7(7)
OT2	0.2764(16)	0.452(4)	0.122(3)	3.0(8)

[a] Esd's refer to last digits printed. Anisotropic thermal parameters are available as supplementary material.

Table 3. Refined Atomic Coordinates and Thermal Parameters for (Cs,K)TA Sample 1

	x	y	z	B_{iso}
	(a) 20 °C			
Cs1	0.3816(1)	0.7773(2)	0.6661(3)	3.34(8)
Cs2	0.1054(1)	0.6778(1)	0.9126(2)	1.59(3)
Ti1	0.3730(1)	0.4886(2)	0.0000	0.66(5)
Ti2	0.2548(1)	0.2570(3)	0.7435(3)	0.65(5)
As1	0.5033(1)	0.3279(1)	0.7400(2)	0.61(3)
As2	0.3184(1)	0.9907(1)	0.9868(2)	0.61(3)
O1	0.4883(6)	0.4704(13)	0.8651(8)	1.3(3)
O2	0.5144(6)	0.4757(14)	0.6135(8)	1.5(3)
O3	0.4033(5)	0.1803(12)	0.7125(7)	1.1(2)
O4	0.1069(5)	0.3143(11)	0.7527(7)	1.0(2)
O5	0.3866(5)	0.7881(9)	0.9517(7)	0.9(2)
O6	0.6096(6)	0.8109(11)	0.5201(8)	1.3(3)
O7	0.2474(6)	0.0330(11)	0.8596(7)	1.0(2)
O8	0.2641(6)	0.4461(13)	0.6007(8)	1.2(3)
OT1	0.2207(5)	0.0388(12)	0.6050(7)	1.0(2)
OT2	0.2865(5)	0.4353(11)	0.8549(8)	1.0(2)
	(b) 222 °C			
Cs1	0.3834(3)	0.7797(5)	0.6512(6)	5.50(20)
Cs2	0.1062(1)	0.6832(2)	0.9005(4)	2.98(7)
Ti1	0.3727(2)	0.4877(5)	0.0000	0.96(11)
Ti2	0.2564(2)	0.2548(5)	0.7401(5)	0.97(10)
As1	0.5048(1)	0.3269(2)	0.7391(4)	0.89(7)
As2	0.3195(1)	0.9886(3)	0.9853(4)	0.92(6)
O1	0.4901(10)	0.464(3)	0.865(1)	1.9(6)
O2	0.5165(10)	0.480(2)	0.618(1)	2.0(6)
O3	0.4059(9)	0.179(2)	0.707(2)	1.8(5)
O4	0.1091(9)	0.314(2)	0.751(1)	1.4(5)
O5	0.3874(10)	0.785(2)	0.951(1)	1.7(5)
O6	0.6113(10)	0.812(2)	0.524(2)	2.0(6)
O7	0.2508(10)	0.032(2)	0.855(1)	2.0(6)
O8	0.2638(9)	0.443(2)	0.597(1)	1.4(5)
OT1	0.2217(10)	0.039(2)	0.602(1)	1.5(5)
OT2	0.2886(9)	0.432(2)	0.852(1)	1.5(5)
	(c) 400 °C			
Cs1	0.3872(2)	0.7880(3)	0.6327(6)	7.2(2)
Cs2	0.1083(1)	0.6933(3)	0.8936(4)	4.9(1)
Ti1	0.3724(1)	0.4955(4)	0.00000	1.40(7)
Ti2	0.2448(2)	0.7594(4)	0.2450(5)	1.35(7)
As1	0.5034(1)	0.3267(2)	0.7430(4)	1.26(4)
As2	0.3210(1)	0.9937(2)	0.9887(3)	1.30(4)
O1	0.4886(10)	0.469(3)	0.867(1)	2.8(6)
O2	0.5166(11)	0.473(2)	0.618(1)	2.7(5)
O3	0.4019(9)	0.187(2)	0.714(2)	2.8(6)
O4	0.1051(9)	0.319(2)	0.760(1)	2.0(5)
O5	0.3892(10)	0.794(2)	0.952(1)	2.5(5)
O6	0.6119(10)	0.803(2)	0.527(2)	2.9(6)
O7	0.2506(9)	0.039(2)	0.860(1)	2.5(5)
O8	0.2611(9)	0.447(2)	0.603(1)	2.1(4)
OT1	0.2202(9)	0.045(2)	0.607(1)	1.9(4)
OT2	0.2856(8)	0.437(2)	0.857(1)	2.1(4)
	(d) 550 °C			
Cs1	0.3884(4)	0.7919(7)	0.6255(12)	8.0(4)
Cs2	0.1095(3)	0.6994(7)	0.8872(11)	6.4(2)
Ti1	0.3722(2)	0.5000(9)	0.0000	1.8(2)
Ti2	0.2537(4)	0.2595(8)	0.7468(11)	1.8(1)
As1	0.5024(2)	0.3272(2)	0.7446(9)	1.6(1)
As2	0.3216(1)	0.9960(5)	0.9910(7)	1.7(1)
O1	0.490(2)	0.475(3)	0.868(2)	3.1(10)
O2	0.517(2)	0.467(5)	0.620(2)	3.6(12)
O3	0.398(2)	0.191(3)	0.720(3)	2.9(12)
O4	0.102(2)	0.320(3)	0.765(3)	2.7(10)
O5	0.388(2)	0.800(4)	0.953(2)	2.6(9)
O6	0.612(2)	0.802(3)	0.527(3)	4.2(14)
O7	0.250(2)	0.045(4)	0.864(2)	3.4(10)
O8	0.258(2)	0.451(4)	0.608(2)	2.6(9)
OT1	0.217(2)	0.048(3)	0.609(2)	2.3(8)
OT2	0.281(2)	0.437(4)	0.860(2)	2.2(8)

[a] Refined occupancies of Cs1 at each temperature are 0.33(1), 0.31(2), 0.50(3), and 0.55(5) Cs and 0.67(1), 0.69(2), 0.50(3), and 0.45(5) K; those for Cs2 are 0.92(1), 0.91(2), 0.70(2), and 0.64(4) Cs and 0.08(1), 0.09(2), 0.30(2), and 0.34(4) K.
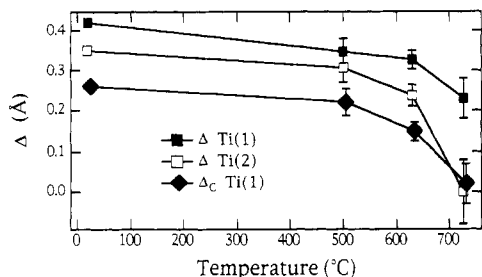
cis-(Ti–O) bond distances connected to two adjacent TiO$_6$ octahedra within the chain) does become equal to zero at the phase transition (Figure 3). Therefore, Δ_cTi(1) better

describes a possible order parameter for the displacement of Ti(1) as the phase transition in KTA is approached.

438 *Chem. Mater., Vol. 6, No. 4, 1994*

Northrup et al.

Figure 3. Titanium octahedral distortion for KTA as a function of temperature. Δ = long *trans*-(Ti–O) minus short *trans*-(Ti–O) distances as defined by Stucky et al.[2] Δ_c = difference between in-chain *cis*-(Ti–O) bonds (see text, Figure 4).
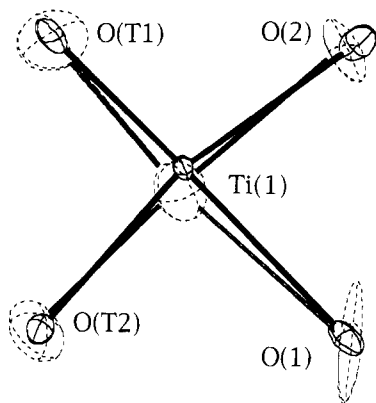
Figure 4. ORTEP[16] diagram of the local Ti(1) coordination of KTA projected down *b*, at 25 °C (solid lines) and 725 °C (dashed). O(5) and O(6) are not shown; thermal ellipsoids (50% probability) are outlined. This projection shows the approach of Ti(1) to a point equidistant between O(T1) and O(T2), rather than to the center of the *trans*-O(T1)–Ti(1)–O(1) linkage.

Table 4. Thermal Expansion Data for KTA and (Cs,K)TA

	$\alpha(a) \times 10^{-5}$ K^{-1}	$\alpha(b) \times 10^{-5}$ K^{-1}	$\alpha(c) \times 10^{-5}$ K^{-1}	$\alpha(V) \times 10^{-5}$ K^{-1}
KTA (20–725 °C)	1.29(2)	1.58(4)	−0.65(9)	2.34(2)
(Cs,K)TA (20–650 °C)	1.20(1)	3.06(2)	−1.52(4)	2.68(2)

Furthermore, Δ_cTi(1) calculated for the analogue TTP above its T_c is zero.

The mean linear and volumetric coefficients of thermal expansion were calculated[17] in the temperature ranges studied from data presented in Figure 2. Temperature has approximately twice the effect on *b* and *c* of (Cs,K)TA compared to KTA, while thermal expansion along *a* ($\alpha_{(a)}$) is relatively unaffected by Cs substitution (Table 4). The unusual behavior of the *c* cell dimension (negative $\alpha_{(c)}$) is related to structural details discussed below. It is noteworthy that although *a*, *b*, and cell volume are larger in (Cs,K)TA, *c* is smaller. Interatomic distances are given in Table 5 (Table 6, interatomic angles, is available as supplementary material).

The negative thermal expansion in the *c* direction is associated with tilting of the framework polyhedra. For the purpose of explaining this structural distortion, the framework of KTA can be considered to consist of layers stacked along *a*. One such layer is depicted in Figure 5, and is made up of Ti octahedral chains along [011] connected by As(2) tetrahedra. The adjacent layer (one-half unit cell along *a*) has the opposite orientation, giving

(17) Hazen, R. M.; Finger, L. W. *Comparative Crystal Chemistry*; Wiley: New York, 1982.

the overall projection along *a* the appearance of a diagonal gridwork. Each layer is strongly connected to the next by As(1) tetrahedra. Figure 6 shows this linkage between the somewhat corrugated layers, in the *ac* plane.

As temperature increases, the Ti(2)–As(1) and Ti(1)–As(2) chains along *b* and *a* lengthen. Because of the complex corner linkage of the framework, extension in the *c* direction is inhibited. The essentially fixed sizes of the octahedra and tetrahedra favor polyhedral rotations to accommodate changes in the effective size of the cation. The undulating chains of Ti octahedra along [011] and [01$\bar{1}$] become more linear in the *ab* plane, and more bent in the *ac* plane. This is accompanied by rotation of the As tetrahedra and shearing of the Ti chains parallel to one another. As a result, there is a collapse along *c* as *a* and *b* expand.

Measurement of the Ti octahedral rotations are complicated by internal distortion. In contrast, the As tetrahedra are more rigid units, and their rotation can be measured by relative displacements of the corner oxygen positions on the appropriate axial projection. The As(2) tetrahedron rotates in the *bc* plane with changing temperature. Its tilt angle θ, rotation about the *a* axis, is defined here as the angle of the O(5)–O(6) edge, which links adjacent Ti(1) octahedra, to the *b* axis (Figure 5):

$$\theta = \tan^{-1}[\Delta z[O(5)-O(6)]c/\Delta y[O(5)-O(6)]b]$$

This angle increases in both KTA and (Cs,K)TA as temperature increases (Table 7). Such rotation allows the chains to slide along one another and increase *b* while decreasing *c*.

The As(1) tetrahedron rotates in the *ac* plane. Its rotation about the *b* axis, ϕ, is similarly defined as the angle of the Ti(2)–linking O(3)–O(4) edge to the *a* axis (Figure 6):

$$\phi = \tan^{-1}[\Delta z[O(3)-O(4)]c/\Delta x[O(3)-O(4)]a]$$

The increase in ϕ with temperature in KTA and (Cs,K)-TA is shown in Table 7. This rotation permits the Ti(1) octahedral chains to spread out in the *a* direction, while shortening *c*. The total effect of this complex framework distortion is to accommodate the change in size of the extraframework cation sites. The K/Cs cations occupy cavities between the convoluted layers. These cavities become effectively larger with increasing temperature or with cesium substitution. Increasing temperature or substituting a larger cation will therefore have analogous consequences: the framework will expand and distort through polyhedral rotations.

Substitution of a larger cation enhances the effect of temperature on framework distortion (i.e. the effect on thermal expansion shown in Table 4). The overall state of framework distortion manifests itself in the unit cell proportions, with the ratio *c/a* decreasing with increasing temperature or cation size. This should be applicable as a measure of distortion for other compositions (Table 7). For each framework composition, the *c/a* ratio for stable compounds should fall within a specific range. The upper (and lower) limits of this framework distortion define the stability of the phase and depend on the size and rigidity of the tetrahedral units. Different combinations of temperature and cationic radius are permitted within such limits. Once established, the limits of *c/a* may be used as a guide to predict the stability of various compositions.

Table 5. Interatomic Distances (Å) as a Function of Temperature

KTA

	temp (°C)						temp (°C)			
	20	500	630	725			20	500	630	725
Ti(1)–O(1)	2.144(5)	2.124(15)	2.085(11)	2.18(3)		Ti(1)–O(6)	2.002(5)	2.004(15)	2.019(13)	2.02(3)
Ti(1)–O(2)	1.953(5)	2.000(16)	1.984(16)	1.97(2)		Ti(1)–O(T1)	1.724(5)	1.747(15)	1.759(13)	1.83(2)
Ti(1)–O(5)	2.039(4)	2.072(13)	2.065(10)	2.06(2)		Ti(1)–O(T2)	1.985(5)	1.967(14)	1.908(11)	1.85(2)
mean	1.974	1.986	1.970	1.986						
Ti(2)–O(3)	2.036(4)	2.029(13)	2.011(11)	2.04(2)		Ti(2)–O(8)	1.984(5)	1.969(17)	1.995(13)	1.94(3)
Ti(2)–O(4)	1.983(4)	2.006(12)	2.045(9)	2.01(2)		Ti(2)–O(T1)	2.106(5)	2.088(15)	2.053(14)	1.88(3)
Ti(2)–O(7)	1.972(5)	1.959(17)	1.967(12)	1.97(2)		Ti(2)–O(T2)	1.754(5)	1.768(17)	1.814(13)	1.96(3)
mean	1.972	1.970	1.981	1.97						
As(1)–O(1)	1.669(5)	1.671(16)	1.667(15)	1.69(4)		As(1)–O(3)	1.684(4)	1.690(13)	1.684(10)	1.69(2)
As(1)–O(2)	1.679(5)	1.653(19)	1.673(16)	1.67(2)		As(1)–O(4)	1.683(4)	1.690(12)	1.689(9)	1.70(2)
mean	1.679	1.676	1.678	1.69						
As(2)–O(5)	1.681(4)	1.675(12)	1.683(9)	1.68(2)		As(2)–O(7)	1.680(5)	1.700(16)	1.680(13)	1.67(2)
As(2)–O(6)	1.668(5)	1.677(15)	1.676(12)	1.66(2)		As(2)–O(8)	1.689(5)	1.686(15)	1.672(11)	1.73(3)
mean	1.680	1.684	1.678	1.68						
K(1)–O(1)	2.979(6)	3.20(3)	3.303(23)	3.45(5)		K(1)–O(7)	3.165(6)	3.302(22)	3.358(18)	3.42(4)
K(1)–O(2)	2.828(5)	2.731(22)	2.710(18)	2.74(2)		K(1)–O(8)	2.703(5)	2.752(18)	2.740(15)	2.73(3)
K(1)–O(3)	2.683(4)	2.716(15)	2.741(12)	2.73(3)		K(1)–O(T1)	2.890(5)	2.852(18)	2.846(15)	2.85(2)
K(1)–O(5)	2.883(5)	3.029(22)	3.130(17)	3.27(4)		K(1)–O(T2)	3.099(5)	3.277(21)	3.402(18)	3.56(4)
K(1)–O(6)	3.516(5)	3.384(19)	3.342(16)	3.32(3)						
mean	2.972	3.027	3.064	3.12						
K(2)–O(1)	2.662(5)	2.654(18)	2.692(17)	2.54(4)		K(2)–O(7)	2.907(5)	2.883(18)	2.885(14)	2.87(3)
K(2)–O(2)	2.969(6)	3.18(3)	3.280(23)	3.37(3)		K(2)–O(8)	3.127(6)	3.230(24)	3.224(20)	3.32(4)
K(2)–O(3)	3.149(6)	3.316(22)	3.319(20)	3.31(4)		K(2)–O(T1)	3.161(5)	3.258(19)	3.352(17)	3.49(3)
K(2)–O(4)	3.061(5)	2.969(16)	2.946(13)	2.99(3)		K(2)–O(T2)	2.854(5)	2.860(18)	2.867(15)	2.82(3)
K(2)–O(5)	2.836(5)	2.890(13)	2.881(12)	2.90(2)						
mean	2.970	3.027	3.050	3.07						

(Cs,K)TA

|	temp (°C)						temp (°C)			
	20	222	400	550			20	222	400	550
Ti(1)–O(1)	2.123(8)	2.130(14)	2.119(14)	2.12(2)		Ti(1)–O(6)	2.031(8)	2.048(13)	2.053(12)	2.08(2)
Ti(1)–O(2)	1.954(8)	1.971(14)	1.962(16)	1.98(3)		Ti(1)–O(T1)	1.723(8)	1.720(13)	1.721(12)	1.70(2)
Ti(1)–O(5)	2.081(7)	2.074(13)	2.100(13)	2.11(3)		Ti(1)–O(T2)	1.979(8)	1.971(13)	1.963(12)	1.97(2)
mean	1.982	1.986	1.986	1.99						
Ti(2)–O(3)	2.078(7)	2.094(13)	2.055(12)	2.01(2)		Ti(2)–O(8)	1.998(8)	1.992(14)	1.981(13)	1.97(2)
Ti(2)–O(4)	2.016(7)	2.014(12)	2.057(12)	2.09(2)		Ti(2)–O(T1)	2.139(8)	2.123(14)	2.123(13)	2.12(2)
Ti(2)–O(7)	1.957(8)	1.946(15)	1.934(14)	1.92(3)		Ti(2)–O(T2)	1.747(8)	1.746(15)	1.744(13)	1.75(3)
mean	1.989	1.986	1.982	1.98						
As(1)–O(1)	1.666(8)	1.653(15)	1.650(15)	1.67(2)		As(1)–O(3)	1.689(7)	1.691(12)	1.685(13)	1.70(2)
As(1)–O(2)	1.693(8)	1.670(14)	1.675(17)	1.65(3)		As(1)–O(4)	1.686(7)	1.693(12)	1.693(12)	1.68(2)
mean	1.684	1.677	1.676	1.67						
As(2)–O(5)	1.678(7)	1.685(13)	1.676(12)	1.65(2)		As(2)–O(7)	1.693(8)	1.697(16)	1.699(13)	1.70(3)
As(2)–O(6)	1.680(8)	1.680(13)	1.692(13)	1.68(2)		As(2)–O(8)	1.678(8)	1.668(13)	1.674(12)	1.67(2)
mean	1.682	1.682	1.685	1.68						
Cs(1)–O(1)	3.297(9)	3.439(18)	3.572(18)	3.63(3)		Cs(1)–O(7)	3.242(8)	3.288(16)	3.484(13)	3.60(2)
Cs(1)–O(2)	2.749(9)	2.711(16)	2.752(14)	2.80(3)		Cs(1)–O(8)	2.809(8)	2.831(14)	2.879(15)	2.91(3)
Cs(1)–O(3)	2.761(8)	2.768(14)	2.845(14)	2.90(2)		Cs(1)–O(T1)	2.850(8)	2.828(14)	2.849(13)	2.89(2)
Cs(1)–O(5)	3.083(8)	3.216(17)	3.416(16)	3.49(3)		Cs(1)–O(T2)	3.319(9)	3.421(15)	3.642(15)	3.77(2)
Cs(1)–O(6)	3.437(9)	3.348(15)	3.220(15)	3.19(2)						
mean	3.061	3.094	3.184	3.24						
Cs(2)–O(1)	2.875(8)	2.859(15)	2.805(15)	2.74(2)		Cs(2)–O(7)	3.097(7)	3.077(13)	3.040(15)	3.02(3)
Cs(2)–O(2)	3.353(10)	3.484(17)	3.486(14)	3.52(3)		Cs(2)–O(8)	3.224(9)	3.247(16)	3.320(14)	3.42(3)
Cs(2)–O(3)	3.238(8)	3.293(16)	3.426(19)	3.56(3)		Cs(2)–O(T1)	3.253(8)	3.307(14)	3.391(13)	3.47(2)
Cs(2)–O(4)	2.984(8)	2.957(13)	2.911(13)	2.89(2)		Cs(2)–O(T2)	2.981(7)	3.013(13)	2.970(13)	2.93(2)
Cs(2)–O(5)	2.963(7)	2.985(13)	3.003(13)	3.06(2)						
mean	3.108	3.136	3.150	3.18						

Although it was not possible to obtain data for either the high-temperature KTA or (Cs,K)TA phase in this study, sufficient information was obtained to clearly project the structural and symmetry changes involved. Small shifts in the Ti and O positions, rotations of the As tetrahedra, and large changes in the K positions (Table 2) are all consistent with the approach to *Pnan* symmetry. The observation of selected diffraction peaks provides further evicence for the *Pna2₁* to *Pnan* transition. While the intensities of all reflections decrease upon heating, those expected to vanish at the phase transition weakened dramatically above 500 °C in KTA and 300 °C in (Cs,K)TA. Such behavior is consistent with the appearance of an n-glide parallel to c.[18] (Cs,K)TA is expected to undergo this transition at a lower T_c than KTA. In fact, the transition-sensitive intensities for (Cs,K)TA decrease at lower temperatures than those for KTA.

(18) Hahn, T., Ed. *International Tables for Crystallography, Vol. A*; D. Reidel: Boston, 1983.
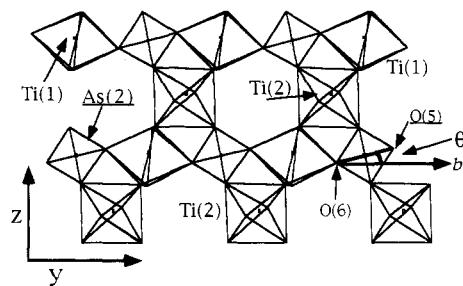
Figure 5. KTA structure viewed along a, at $0 < x < 0.5$, showing the tilt angle θ for As(2) tetrahedra. The titanium octahedral chains are along [011]. At $0.5 < x < 1.0$, this figure is reversed, so that the octahedral chains are along [01$\bar{1}$].
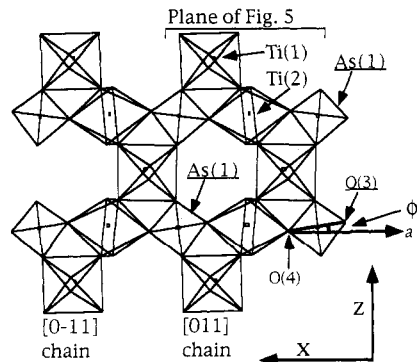

Figure 6. KTA structure projected along b, showing the tilt angle ϕ for As(1) tetrahedra. The titanium octahedral chains alternate along [011] and [01$\bar{1}$] and thus are inclined to the plane shown.

Table 7. Tetrahedral Tilt Angles θ and ϕ for KTA and (Cs,K)TA at Increased Temperatures[a]

compound	temp, °C	θ (deg)	ϕ (deg)	c/a
NaTA	20	13.3	6.9	0.839
KTA	20	14.7	8.7	0.822
	500	16.4	9.3	0.814
	630	15.6	9.9	0.812
	725	16.6	10.0	0.810
TTA	20			0.812
(Cs,K)TA	20	15.3	9.1	0.807
	220	16.2	9.9	0.802
	400	16.3	10.2	0.798
	550	16.3	10.0	0.796
CsTA	20			0.792

[a] Values for NaTA ($Na_{0.87}K_{0.13}TiOAsO_4$) at room temperature are calculated from ref 5; those for TTA and CsTA are calculated from refs 2 and 6. A practical measure of this framework distortion is the axial ratio c/a (see text). Data are listed with increasing cation-site size. Errors for θ and ϕ are $\pm 0.3°$.

Exchange occurs between the M(1) and M(2) sites above 500 °C in (Cs,K)TA; refined Cs occupanices converge substantially (Figure 7). Such disordering is required for the phase transition—the two sites are equivalent in *Pnan*. However, the small crystal sample of (Cs,K)TA used in this study was not stable to temperatures above 550 °C. It underwent a chemical change, apparently losing Cs. While the TiOAsO$_4^-$ framework in part of the crystal remained intact, and maintained its crystallographic orientation, the more volatile Cs diffused out and K diffused in, until the diffraction pattern matched that of KTA. This change occurred slowly enough to be monitored in situ by unit cell measurements, but constant change prevented collection of structural data with this apparatus. Since KTA has a higher T_c than (Cs,K)TA, this reaction competes with the phase transition, and pushes the
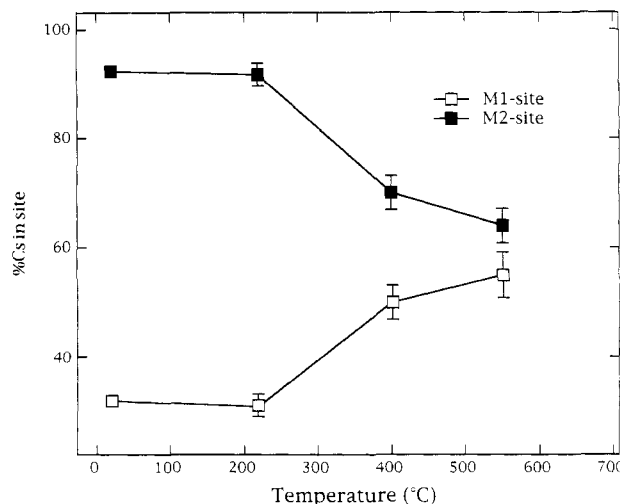
Figure 7. Cesium occupancy factors for M1 and M2 sites in (Cs,K)TA (Table 3). The remainder of each site contains potassium.

transition temperature higher in the K-enriched phase. For bulk (~ 0.5 cm^3) crystal samples tested, this decomposition was not significant. The compositional changes emphasize the increase in cation mobility with temperature, the stability of the framework, and the role of cationic radius in determining the framework distortion and phase relations.

Conclusions

High-temperature single-crystal X-ray diffraction techniques have proven useful in this study, enabling investigation of the effects of temperature on bond configurations, cell parameters, framework distortions, cation distribution, and symmetry. All evidence supports *Pnan* as the high-temperature space group of both KTA and CTA. With regard to the *Pna2$_1$* to *Pnan* phase transition itself, distortions *within* the TiO$_6$ octahedra, which are associated with NLO properties, decreases as a function of temperature. However, the mode of symmetrization differs between Ti(1) and Ti(2). Measurements of framework polyhedral rotations indicates that increasing temperature and substitution of larger cations are analogous, in agreement with the fact that the phase transition temperature, T_c, decreases with increasing cation size. The linear and volumetric coefficients of thermal expansion show temperature to have a greater effect on (Cs,K)TA than on KTA, accounting for the observation that cation ordering is present in (Cs,K)TA only at temperatures below about 550 °C. Finally, the unit-cell ratio c/a may be regarded as a practical and useful indicator of framework deformation and, ultimately, phase stability.

Supplementary Material Available: Table 6, bond angles for KTA and (Cs,K)TA at each temperature studied, and Tables 8 and 9, anisotropic thermal parameters for KTA and (Cs,K)TA, respectively, at each temperature (10 pages). Ordering information is given on any current masthead page.